Drought stress variability in ancient Near Eastern agricultural systems evidenced by $\delta^{13}C$ in barley grain

Simone Riehl[a,b,1], Konstantin E. Pustovoytov[c], Heike Weippert[c], Stefan Klett[a], and Frank Hole[d]

[a]Institute for Archaeological Science and [b]Senckenberg Center for Human Evolution and Palaeoecology, University of Tübingen, 72070 Tübingen, Germany; [c]Institute of Soil Science and Land Evaluation, University of Hohenheim, 70593 Stuttgart, Germany; and [d]Department of Anthropology, Yale University, New Haven, CT 06511

Edited by Kent V. Flannery, University of Michigan, Ann Arbor, MI, and approved July 17, 2014 (received for review May 22, 2014)

The collapse and resilience of political systems in the ancient Near East and their relationship with agricultural development have been of wide interest in archaeology and anthropology. Despite attempts to link the archaeological evidence to local paleoclimate data, the precise role of environmental conditions in ancient agricultural production remains poorly understood. Recently, stable isotope analysis has been used for reconstructing site-specific ancient growing conditions for crop species in semiarid and arid landscapes. To open the discussion of the role of regional diversity in past agricultural production as a factor in societal development, we present 1.037 new stable carbon isotope measurements from 33 archaeological sites and modern fields in the geographic area of the Fertile Crescent, spanning the Aceramic Neolithic [10,000 calibrated years (cal) B.C.] to the later Iron Age (500 cal B.C.), alongside modern data from 13 locations. Our data show that drought stress was an issue in many agricultural settlements in the ancient Near East, particularly in correlation with the major Holocene climatic fluctuations, but its regional impact was diverse and influenced by geographic factors. Although cereals growing in the coastal areas of the northern Levant were relatively unaffected by Holocene climatic fluctuations, farmers of regions further inland had to apply irrigation to cope with increased water stress. However, inland agricultural strategies showed a high degree of variability. Our findings suggest that regional differences in climatic effects led to diversified strategies in ancient subsistence and economy even within spatially limited cultural units.

Holocene climate change | agricultural societies | aridity stress | Middle East | archaeobotanical crop species

The emergence and decline of early civilizations is intrinsically tied to agricultural surplus production, either enabling a focus on technological progress and the accumulation of wealth or, in the case of insufficient yield, leading to hunger, violence, and war.

Although the role of agriculture in state building is uniformly accepted, the role of climate in agricultural production and societal development in the ancient Near East has been explained in radically different ways, closely related to the scientific background and the humanistic mindset of the individual researchers. Environmental versus cultural determinism are competing explanatory models of societal change (1, 2). However, neither model adequately accommodates the multicausal structure of responses of human societies to high variability in natural and process-related effects (3, 4).

Local effects of global Holocene climatic fluctuations have been recognized with diverse magnitudes in paleoclimate proxy archives in the Near East (5–11). Among these climatic shifts, the 4200 B.P. event has been most intensively discussed by archaeologists and geographers, who have linked this fluctuation to the decline of state systems at the end of the Early Bronze Age (12–16). Societal collapse has been supported by evidence of population movements into more favorable regions (17, 18). Agricultural production at the transition from the Early to the Middle Bronze Age shows regionally limited changes in preferred crop species, which are interpreted as being related to increased aridity at the end of the third millennium calibrated years (cal) B.C. (4, 19).

Although paleoenvironmental studies and archaeological records imply that droughts had a major impact on ancient agricultural yields (20), these data only indirectly reflect agricultural production. At present, the only way to directly link climatic fluctuations and agricultural productivity in the past is through stable carbon isotope analysis of archaeological plant remains. This method is an established tool for identifying ancient environmental conditions for plant growth in arid to semiarid environments because $\delta^{13}C$ values in cereals provide a drought-stress signal when the amount of water received during the grain-filling period is low (21–26). Carbon fixation during photosynthesis leads to typical ranges of $\delta^{13}C$ between −28‰ and −25‰ in modern barley, which is a C3 plant (27). In case of drought stress, the plants protect themselves from dehydration through closure of the stomata, which leads to a relative enrichment of the heavy vs. the light carbon isotope in the plant tissues (22).

Because the $\delta^{13}C$ signal reflects seasonal fluctuations in moisture conditions, we undertook stable carbon isotope analysis of archaeological and modern barley grains to assess the impact of known Holocene climatic fluctuations on agricultural and economic dynamics in ancient societies. Here, we present a reconstruction of the effects of past climatic fluctuations on cereal agriculture in the ancient Near East, expressed as chronological sequences and spline interpolation maps of isolines of stable carbon isotope means and minima. Our calculations are based on 1.037 $\delta^{13}C$ measurements from individual barley grains derived from 33 archaeological sites and 13 modern locations (Fig. 1, Table S1, and *Materials and Methods*).

Significance

Collapse and resilience of ancient Near Eastern societies is intrinsically tied to agricultural production. Despite intensive palaeoclimate research, the role of environmental conditions in ancient agricultural production is little understood. Stable carbon isotope analysis on cereal grains from archaeological sites provides a direct evidence for drought stress. This paper demonstrates that drought stress correlated with major climatic fluctuations and affected many agricultural settlements in the ancient Near East but that its regional impact was diverse and influenced by geographic factors and human technology. The results lead to a better understanding of how ancient agricultural societies performed under fluctuating climate and regionally diverse environmental conditions.

Author contributions: S.R. designed research; S.R. performed research; K.E.P., H.W., S.K., and F.H. contributed new reagents/analytic tools; S.R. analyzed data; and S.R. wrote the paper.

The authors declare no conflict of interest.

This article is a PNAS Direct Submission.

Freely available online through the PNAS open access option.

[1]To whom correspondence should be addressed. Email: simone.riehl@uni-tuebingen.de.

This article contains supporting information online at www.pnas.org/lookup/suppl/doi:10.1073/pnas.1409516111/-/DCSupplemental.

Our working hypothesis is that, even with the limitations in the scope of this study (i.e., we do not consider sociocultural issues that influenced agricultural decision making), large-scale stable carbon isotope analysis of ancient cereal grains contributes to our understanding of how agricultural societies performed under fluctuating climate and regionally diverse environmental conditions.

Results and Discussion

Dynamics of Regional Drought Stress Within the Framework of General Climate Trends. Although in arid to semiarid environments other factors, such as crop density and soil salinity, may play a role in causing a drought stress signal in the plant, the strongest correlation of stable carbon isotope data in plants exists with water availability (27–29). Variability of $\delta^{13}C$ measurements in archaeobotanical cereal grains occurs at different levels. In arid environments the variability of $\delta^{13}C$ values may be higher than in semiarid or subhumid regions. Moreover, irrigation can lead to locally diverse water availability for cereal crops and thus to a broad range of values from an individual archaeological site (30) or between different sites (31). In our study, some samples from where irrigation is known along the Euphrates produced a comparatively large range of $\delta^{13}C$. This large range of $\delta^{13}C$ may have resulted from selective irrigation on some fields and not on others (e.g., Emar and Tell el'Abd) (see Fig. 3). Intersite or regional variation of $\delta^{13}C$ in ancient cereal grains has also been interpreted as reflecting differences in growing conditions, resulting from interannual variation in precipitation or from paleoclimatic fluctuations (29, 32, 33). A major problem is that the practice of irrigation remains uncertain for most archaeological sites. We tried to overcome this problem by including minima values of $\Delta^{13}C$ indicating the maximum stress measured. The $\Delta^{13}C$ refers to calibrated $\delta^{13}C$ values. Calibration is necessary due to changes in the atmospheric CO_2 concentration ($\delta^{13}C$ air) over time (for details see *Materials and Methods*). The minima values of $\Delta^{13}C$ represent those crops that probably were not irrigated, even in settlement areas with locally irrigated fields (see Figs. 3 and 5). However, to unambiguously interpret $\delta^{13}C$ values from a Near Eastern Bronze Age site as being related to irrigation, additional archaeobotanical (e.g., weed species), archaeological, and geoarchaeological data and textual evidence need to be incorporated, which currently is only feasible for a few archaeological sites (30, 34).

Our results of accumulated $\delta^{13}C$ data document for the first time, to our knowledge, a generalized trend in water availability for the area of the Fertile Crescent over a time sequence spanning from the Neolithic to the Iron Age (Fig. 2). This accumulated trend was calculated from the means (Table S1 and Fig. 3) of the 33 archaeological sites depicted (Fig. 1). Fig. 2 shows the chronological course of the $\Delta^{13}C$ values fluctuating roughly between 15‰ and 18‰. Values below the reference line of 16‰ indicate strong water stress, and values of 16‰ to 17‰ note moderate stress (see *Materials and Methods* for the basis of these reference values).

The generalized $\Delta^{13}C$ trend is in good agreement with known Holocene climatic fluctuations, particularly regarding those of 5200 B.P., 4200 B.P., and 3200 B.P. (9, 35–38) (Fig. 2). We also recognize fluctuations within the sequence of the Early Bronze Age that are in line with opinions on locally variable climatic effects and settlement patterns during the Early Bronze Age (39–42). During the Neolithic and Chalcolithic periods, water availability seems to have been comparatively more balanced and in agreement with other paleoclimate records (43–45), although not free of fluctuations (9).

Bearing in mind the modern differences in Near Eastern climatic geography, deviations in water availability from the general trend as seen in the accumulated $\Delta^{13}C$ record should become visible at a regional level. For testing this hypothesis, we defined four geographical regions (Fig. 3): coastal sites, which receive relatively stable interannual levels of high precipitation; Euphrates sites, situated in the drier inland but with the option for farmers to access the permanent water course of a major river; Khabur sites, with a relatively strong north–south decline, the northern sites being close to the Taurus mountains and the southern sites having occasional access to irrigation water from the Khabur and its tributaries; and sites neither on the coast nor along one of the large rivers.

The regional development of the $\Delta^{13}C$ record confirms the expectation of differences according to geographical units (Fig. 3). From the coastal sites, the minima rarely plot below the 16‰ reference line, and the mean value is in most cases on or above the 17‰ line, indicating that drought stress was not a major problem to the farmers in this region at any time of the considered sequence. Even during the major climatic fluctuations of 4200 B.P. and 3200 B.P., drought stress on barley was only moderate in most coastal sites. These patterns are in contrast to the Euphrates and Khabur river systems, where the minima of $\Delta^{13}C$ reach 13‰ and the mean values are rarely above 17‰. From the Euphrates sites, a particularly large number of $\Delta^{13}C$ values are below the 16‰ reference line during the Middle

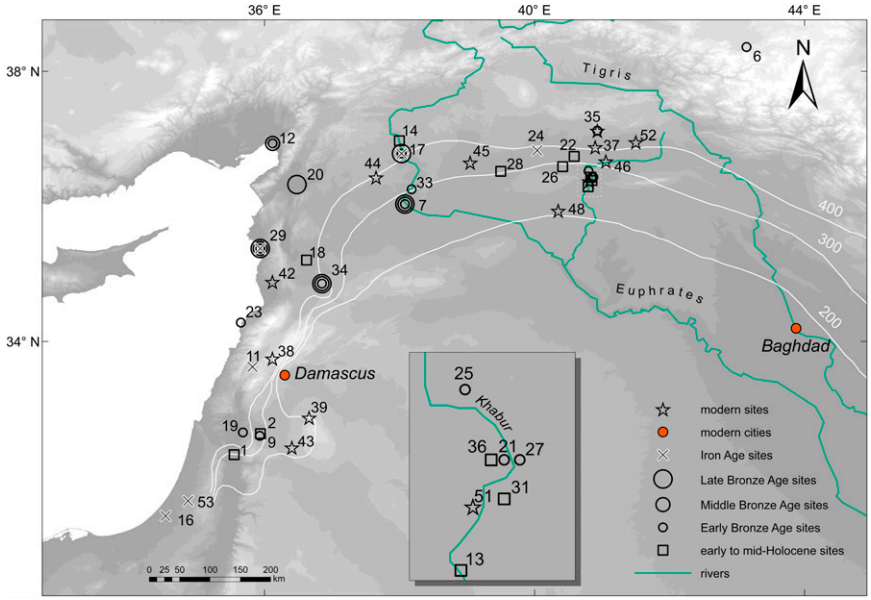

Fig. 1. Sampling locations in northern Mesopotamia and the Levant and chronology of barley grains providing $\delta^{13}C$ measurements. Note that the only sites listed are those that appear in the map section: (site 1) Abu Hamid, (site 2) Ain Rahub, (site 6) Dilkaya Höyük, (site 7) Emar, (site 9) Hirbet ez-Zeraqon, (site 11) Kamid el-Loz, (site 12) Kinet Höyük, (site 13) Mashnaqa, (site 14) Mezraa Teleilat Höyük, (site 16) Qubur al-Walayida, (site 17) Tell Shioukh Faouqani, (site 18) Shir, (site 19) Tell esh-Shuna, (site 20) Tell Atchana, (site 21) Tell Atij, (site 22) Tell Beydar III, (site 23) Tell Fadous, (site 24) Tell Halaf, (site 25) Tell Kerma, (site 26) Tell Kuran, (site 27) Tell Raqa'i, (site 28) Tell Tawila, (site 29) Tell Tweini, (site 31) Umm Qseir, (site 33) Tell 'el Abd, (site 34) Qatna, (site 35) Tell Mozan, (site 36) Ziyade, (site 37) Chagar Bazar, (site 38) Zebdani (GPS_152), (site 39) GPS_17, (site 42) Tell Snan (GPS_437), (site 43) Summakiak (GPS_50), (site 44) Membij (GPS_629), (site 45) Tell Abyad (GPS_755), (site 46) Tell Brak (GPS_828), (site 48) Malhat ed Deru, (site 51) Tell Bderi, (site 52) Tell Leilan, and (site 53) Tel Burna. Please note that some of the archaeological sites have been sampled only for modern control $\delta^{13}C$. For details on the sites and samples, see Table S1.

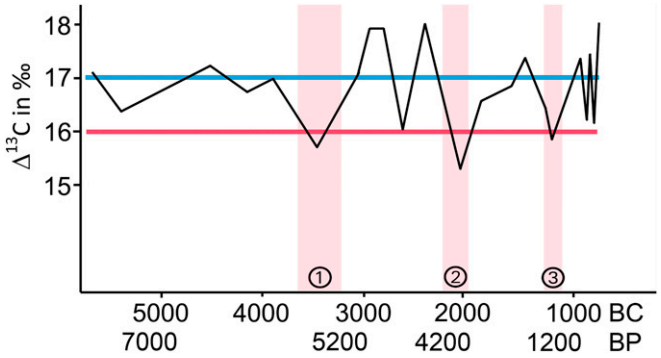

Fig. 2. Accumulated $\Delta^{13}C$ mean record from 1.037 barley grains from 33 archaeological sites (black line). Red line, reference line for drought stress at 16‰ and below; blue line, reference line for favorable conditions at 17‰ and above; red bars, global climatic fluctuations at roughly 5200 B.P. (①), 4200 B.P. (②), and 3200 B.P. (③).

Bronze Age. All regions at some distance from the coast show a strong to moderate stress signal for the major climate events. The reason for a moderate stress signal at Tell Mozan at the 4200 B.P. event is open for debate; it could be because of seasonally higher precipitation due to the close vicinity of the Taurus mountains or because irrigation played a role.

Isolines of $\Delta^{13}C$ Show Spatial Patterns of Drought Stress in the Past. A significant result of this study is the locally highly variable drought-stress signals found under continental climate conditions, due to comparatively higher aridity inland than along the coast (Fig. 4). The option of irrigation, particularly along the rivers, results in assemblages containing both grains from former stands that had been irrigated and others that grew without irrigation, leading to a broad range of $\Delta^{13}C$ values. This relation has been captured by spline interpolation of the differences between mean and minima $\Delta^{13}C$ values from the different locations (Fig. 4). The patterns indicate a high variability of $\Delta^{13}C$ values in regions with probable irrigation, inland in the southern Levant and along the rivers, whereas the coastal areas are characterized by low intrasample variability in $\Delta^{13}C$ values. These relationships are relevant to the interpretation of $\Delta^{13}C$ data sets from archaeological sites with unknown agricultural strategies: i.e., where the archaeological evidence for irrigation is pending. These patterns also support the suggestion that high environmental diversity, combined with regionally differing human strategies, are responsible for the heterogeneity of the Near Eastern archaeological and geoarchaeological record (4, 46).

Chronological spline interpolation of $\Delta^{13}C$ values in barley shows distinct and regionally variable differences in drought-stress signals throughout time (Fig. 5). In agreement with earlier local studies (44, 47), the mean values for the Early to Mid-Holocene (10,000–4000 cal B.C.) are considerably higher than modern $\Delta^{13}C$ signals, indicating good water supply for barley growth in areas where this crop species experiences drought stress today, basically around the modern 300-mm isohyet. The differences between the modern and Early to Mid-Holocene $\Delta^{13}C$ record are not so strong regarding the minima, which indicate the highest possible drought stress of individual samples, and are thus generally indicative of the lowermost natural base line of water supply. However, with both interpolations, mean and minima, it is obvious that the area between the modern 200-mm and 300-mm isohyets received considerably higher precipitation during the growing season of the cereals in the Early to Mid-Holocene periods than today.

The conditions during the first half of the Early Bronze Age (4000–2500 cal B.C.) seem to have been slightly drier than before, expressed by lower mean $\Delta^{13}C$ values in the southern region, the Khabur area, and around the modern 400-mm isohyet whereas there may have been some beneficial influence from the waters of the Euphrates at the settlements located along the river. The presence of a coastal site (Tell Fadous) in the first half of the Early Bronze Age is responsible for the contrasting pattern in this area. A north–south declining precipitation gradient is particularly visible in the minima values.

The second half of the Early Bronze Age (2500 to *ca*. 2000 cal B.C.) shows an increase in aridity, particularly at the sites of Qatna and Emar: i.e., south of 36° latitude and south of the modern 300-mm isohyet whereas the mean values north of 36° show a much weaker drought stress signal. Although the general trend was in agreement with the expected effects of the 4200 B.P. event, regional differences in the climatic effects obviously existed (15, 16).

The Middle Bronze Age (*ca.* 1900–1600 cal B.C.) appears to show a continuation of this process, which is particularly visible in the minima values indicating extremes of drought stress in the Khabur area, but also at the sites of Emar and Qatna, whereas only slight changes toward higher aridity occurred along the coast, at Kinet Höyük and Tell Tweini. This increased inland aridity correlates with archaeologically observed demographic patterns in northern Mesopotamia, the Khabur-Balikh steppe, the middle Euphrates (46), and the Aleppo and Hama districts (48). There was a reduction in the number of sites between the end of the Early Bronze Age and the Middle Bronze Age. The mean values for Qatna, which contrast with these patterns, could be explained by irrigation or at least cultivation of some barley fields in the direct vicinity of the paleolake reconstructed for this site (49).

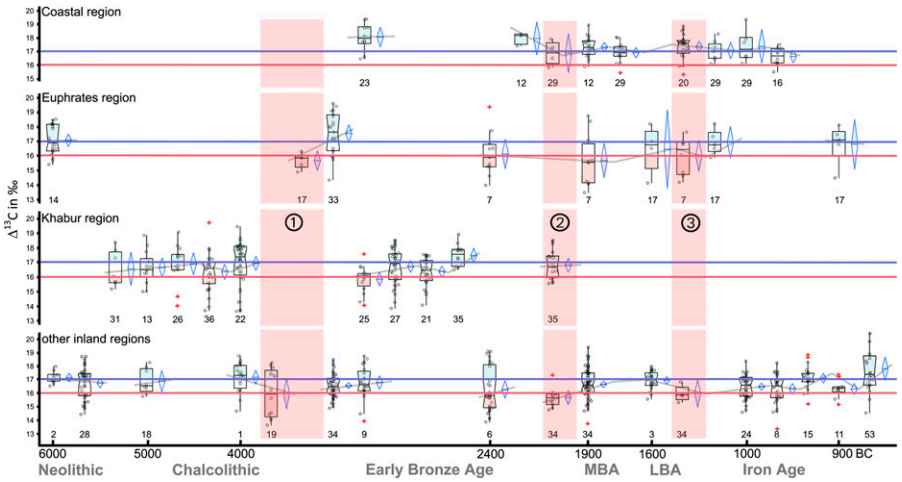

Fig. 3. Regional and local $\Delta^{13}C$ record from 1.037 barley grains from 33 archaeological sites. Each boxplot represents one phase of a site; numbers below the boxplots refer to the archaeological sites in Fig. 1 and Table S1; gray circles are individual measurements; red crosses are outliers; blue diamonds represent means; reference lines and red bars as in Fig. 2. MBA, Middle Bronze Age; LBA, Late Bronze Age.

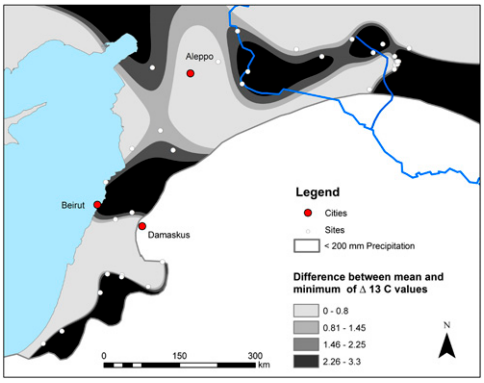

Fig. 4. Differences between mean and minima $\Delta^{13}C$ values in ‰ for all sites (modern, historic, and prehistoric) with more than six measurements, representing the range of variation at the different locations.

The Late Bronze Age (1600–1100 cal B.C.) mean values are very similar to those of the second half of the Early Bronze Age. Compared with the Middle Bronze Age data, the means for most locations show decreased stress signals, except for Qatna, where some drought stress is indicated. Although the latter would fit with other local paleoclimate proxies such as the $\delta^{18}O$ records from Soreq Cave (5) and Lake Van (50), proxy records of higher resolution in the southern Levant (51) and in Anatolia (52) indicate climatic instability in a generally drying trend, with humid episodes during the Late Bronze Age. The minimum value from Qatna shows a decrease in drought stress compared with the Middle Bronze Age, which would support the presence of humid episodes during the Late Bronze Age. As we currently do not have any $\Delta^{13}C$ data from the southern Levant, the role of climatic impact on barley stands in the southern region is impossible to assess.

The Iron Age (1050–500 cal B.C.) patterns are somewhat problematic because no sites are available for interpolation south of the 400-mm isohyet: i.e., the inland locations are not reflected well by the $\Delta^{13}C$ isolines. Comparing the minima values of the southern Levant to the previous periods (MBA and LBA), an increased aridity is indicated.

Overall, the prehistoric and historic mean $\Delta^{13}C$ values show lower stress signals than today whereas the ancient minima $\Delta^{13}C$ values are more similar to modern values. The interpolation of $\Delta^{13}C$ ranges emphasizes shifting isohyets throughout time, with the strongest drought-stress signals occurring between the modern 300- to 200-mm isohyets during the Middle Bronze Age, the second half of the Early Bronze Age, and the Late Bronze Age, in decreasing order. Particularly significant are the changes in drought-stress signals of the Early Bronze Age to Middle Bronze Age sequence, which are in agreement with the changing archaeological settlement record (46, 48) and the paleoclimate proxy records describing the 4200 B.P. event (15).

In general, the $\Delta^{13}C$ values from archaeobotanical barley grains in northern Mesopotamia and the northern Levant are in good agreement with known Holocene climatic fluctuations whereas the regional development shows differences according to geographical units, with better water availability in the coastal region than inland. High variability of $\Delta^{13}C$ values plays a role in settlements where irrigation has been practiced because some cereal stands did not receive additional irrigation water. The diversity of these complex patterns is reflected nicely in the chronological spline interpolation of $\Delta^{13}C$ values.

These new data outline the regional variability of climate-related and anthropogenically modified subsistence conditions

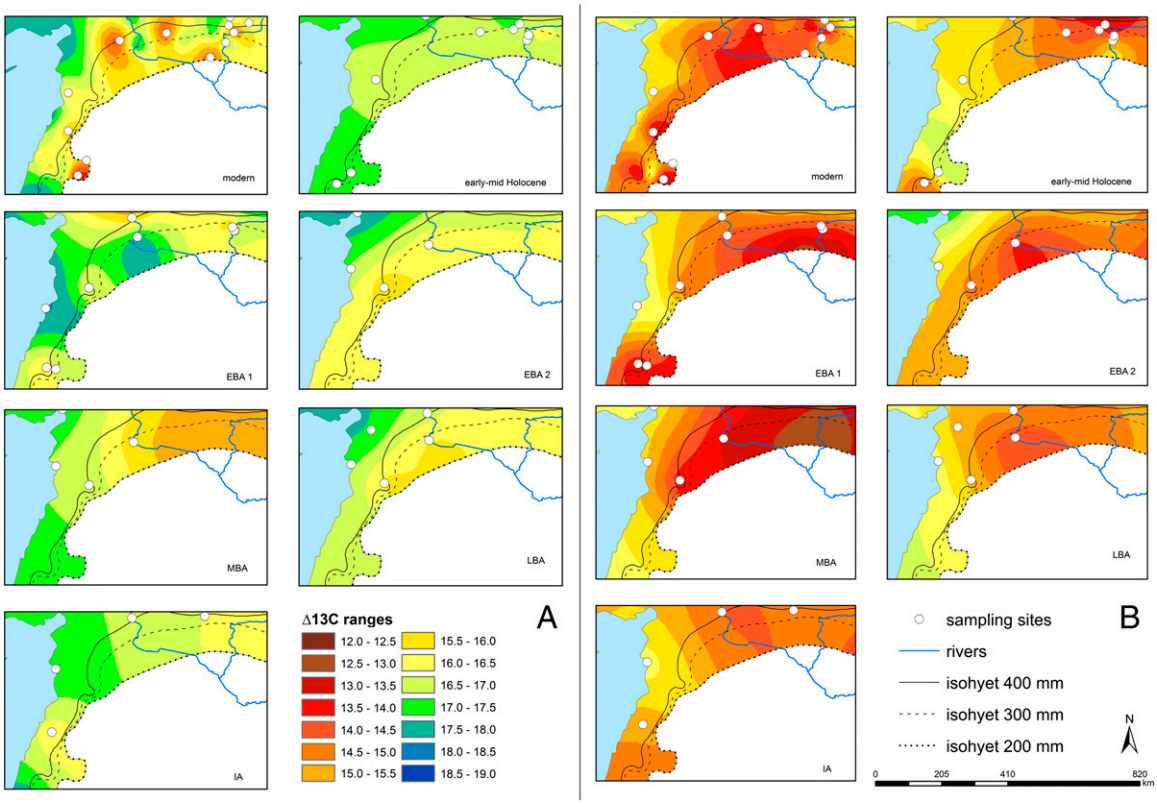

Fig. 5. (*A*) Spline interpolation of mean $\Delta^{13}C$ values from barley grains for different chronological segments. (*B*) Spline interpolation of minima $\Delta^{13}C$ values from barley grains for different chronological segments. Red, strong drought stress; yellow, considerable to slight drought stress; green, moderate drought stress; blue, no drought stress.

throughout the Holocene and thus broaden our understanding of causal relations between environmental dynamics and societal development in the ancient Near East. Although we did not specifically address sociocultural issues that may have influenced agricultural decision making, our results provide a key for answering the pivotal question of how agricultural societies performed under fluctuating climatic and environmental conditions, which also has implications for risk assessment in regions of endangered food security today.

Conclusions

Our results show the regional diversity in climatic effects on ancient crop species in the Near East over the Holocene sequence and support one possible causal motivation for societal transformations in this geographical region.

Under specific types of stress, the interplay between humans and their environment codetermines the resilience, continuity, vulnerability, decline, and regeneration of societies. Although archaeology is currently only at the beginning of disentangling past human–environment interaction, details of environmental change and economic development in ancient societies are now enhancing our understanding of the reasons for variability of feedback mechanisms in human–environment systems. Essentially, the results pinpoint the importance of local variability in terms of action planning.

Materials and Methods

Stable Carbon Isotope Analysis of Archaeobotanical Cereal Grains. Barley grains from 33 archaeological sites (Fig. 1) were analyzed for stable carbon isotope ratios, taking into account knowledge of intraspecific and intrasample variability of $\delta^{13}C$ (23, 53). The described high variability required a target of minimum measurements of six individual grains per archaeobotanical sample, representing a unique contextual unit (Table S1). In some cases, fewer grains per contextual unit were analyzed because of limited availability of material. Well-developed grains were chosen to guarantee the exclusion of $\delta^{13}C$ values that would not reflect the mean growing conditions: e.g., such as values from immature grains.

The geographical distribution of the archaeological sites is in agreement with the western and northern part of the Fertile Crescent, the area that has been a focus for studies on the emergence of agriculture in the Old World and on the development of ancient civilizations. The chronological distribution of the sampled sites is, however, uneven, for reasons of differences in the availability of archaeobotanical barley grains. Although the distribution of modern locations is relatively even, the number of locations for the Middle Bronze Age (*ca*. 1900–1600 cal B.C.) and the Late Bronze Age (*ca*. 1600–1200 cal B.C.) is limited and restricted to the northwestern part of the area investigated (Figs. 1 and 5).

Measurements of $\delta^{13}C$ were carried out at the Institute of Geosciences of the University of Tubingen, Germany on a FinniganMAT252 gas source mass spectrometer with a ThermoFinnigan GasBench II/CTC Combi-Pal autosampler. Before mass-spectrometric measurements, the barley grains were reacted with 5% HCl to eliminate sedimentary carbonate.

The common standard of $\delta^{13}C$ VPDB (Vienna Peedee belemnite ‰) was applied to the measurements of $^{13}C/^{12}C$ ratios to calculate $\delta^{13}C$ in the barley grains. Changes in atmospheric CO_2 concentration ($\delta^{13}C$ air) over time needed to be taken into account when comparing cereal grains from different archaeological periods. Past $\delta^{13}C$ air values are available from ice-core projects in Greenland and Antarctica (54–56). We calibrated our $\delta^{13}C$ from ancient barley into $\Delta^{13}C$ values by using the approximation AIRCO2_LOESS (22, 57).

The reference lines of 16‰ and 17‰ have to be considered as relative borders (Figs. 2 and 3), depending also on δ_{air} when calibrated from the negative $\delta^{13}C$ to the positive $\Delta^{13}C$. Studies on the direct relationship between total water input (TWI) during the grain-filling period and the $\delta^{13}C$ value in modern barley relate values below 50 mm TWI during the grain-filling period to a range of $\delta^{13}C$ between −24‰ and −20‰ (58). Considering the grain-filling period of barley to be shorter than 40 d, a TWI of about 40 mm would equal the monthly precipitation of the spring season in the coastal and hilly regions of our investigation area. In modern barley, 40 mm TWI equals a $\delta^{13}C$ value of roughly −23‰, corresponding to a $\Delta^{13}C$ of roughly 16‰. We therefore consider ancient, calibrated values between 17‰ and 16‰ and below to indicate increasing drought stress.

Interpolation Methods. Plant stable carbon isotope values correlate with rainfall at global and regional scales, with the regional scale producing the stronger correlation (27) as well as throughout time (23). Because there is a positive spatial autocorrelation for precipitation, we assumed a positive spatiotemporal autocorrelation for the $\Delta^{13}C$ values of barley grains (59). Positive spatial autocorrelation postulates correlation between attribute values ($\Delta^{13}C$) depending on their proximity.

Therefore, we considered interpolation methods as appropriate for creating a continuous model surface and for visualizing local variability from discrete observations. In the present study, the discrete observations are represented by the $\Delta^{13}C$ values from barley grains.

From the three different local interpolation methods—inverse distance weighting (IDW), kriging, and spline—we chose the latter for its suitability in retaining small-scale variability in the data. Spline interpolation is a mathematical method of smoothing linear features imposing two conditions. First, the surface must pass exactly through the observed points; second, the surface must have a minimum curvature.

The spline interpolation method estimates values by using piecewise polynomial functions linked together at break points to form a bicubic spline (the extension of cubic interpolation by interpolating value points on a 2D regular grid), resulting in a smooth surface that passes through the known point data (60). Conceptually, the interpolator works like bending a sheet of rubber to pass through a 3D point cloud. In this study, a so-called thin-plate spline interpolation, implemented in *ArcGIS,* was used to replace the exact surface by a weighted average, producing a minimum-curvature surface. The advantage of the thin-plate spline is that no unnatural breaks caused by exceptionally high or low values will occur. The setting of the weight can be either tensioning or regularizing. Here, the spline type "regularized" was applied, adjusting the third derivative in the curvature minimization expression for a smoother surface (61).

Because the regular spline method disregards geographical barriers, such as mountain ranges and alterations in precipitation, a spline-with-barriers routine was applied (62). The spline-with-barriers operator estimates unknown values by curving a surface through known values as well as interruptions by the barriers. In this work, the 200-mm isohyet served as an interpolation barrier (63). The 200-mm isohyet was chosen because no sample locations occur south of it, and it is generally considered to represent the barrier of rain-fed agriculture (48).

The use of the barrier mapping method links the drought stress indicated in the $\Delta^{13}C$ values to major topographical and precipitation rates and provides results that are more robust than those from regular interpolations. The barriers, as a means of drought-stress border, alter the process of interpolation by forcing the trend surface to go around the barrier instead of crossing it (64). The final representation can be used to estimate areas with respectively higher or lower water stress.

The spline-with-barrier interpolation method was performed consistently by using the same algorithm for seven time slices ranging from the Neolithic period to the present (Fig. 5). For each location, mean and minimum values of $\Delta^{13}C$ were used (Table S1). The number of sites per time slice varied from a minimum of 4 for the Middle Bronze Age to 13 for the modern locations. To limit the processing extent of the interpolated surfaces, a data file was created including all sites from all periods within a surrounding rectangle. Color formatting of the $\Delta^{13}C$ isoline ranges (Fig. 5) was conducted according to the physiological reaction of the plants, with values between 11.5‰ and 12.5‰ in brown indicating extreme drought stress, and values between 17.5‰ and 18.5‰ shown in blue, indicating good moisture availability for barley growth.

The interpolation results indirectly show climatic fluctuations throughout the Holocene by visualizing local spatial surface changes of $\Delta^{13}C$ values from barley grains.

ACKNOWLEDGMENTS. The following researchers contributed by generously providing barley grain: Mark Nesbitt, Joy McCorriston, Reinder Neef, Elena Marinova, and Reid Bryson. Financial support was obtained through German Research Foundation Grant Ri 1193/6-1.

1. Weiss H, Bradley RS (2001) Archaeology. What drives societal collapse? *Science* 291(5504):609–610.
2. Yoffee N (2010) *Collapse in Ancient Mesopotamia. What Happened, What Didn't? Questioning Collapse: Human Resilience, Ecological Vulnerability and the Aftermath of Empire*, eds McAnany PA, Yoffee N (Cambridge Univ Press, Cambridge, UK), pp 176–203.
3. Geyer B (2002) Expansion and decline of Syria's arid margin. *Arab World Geographer* 5(2):73–84.

4. Riehl S (2012) Variability in ancient Near Eastern environmental and agricultural development. *J Arid Environ* 86:113–121.
5. Bar-Matthews M, Ayalon A, Kaufman A (1997) Late Quaternary paleoclimate in the Eastern Mediterranean region from stable isotope analysis of speleothems at Soreq Cave, Israel. *Quat Res* 47:155–168.
6. Enzel Y, et al. (2003) Late Holocene climates of the Near East deduced from Dead Sea level variations and modern regional winter rainfall. *Quat Res* 60:263–273.
7. Robinson SA, Black S, Sellwood BW, Valdes PJ (2006) A review of palaeoclimates and palaeoenvironments in the Levant and Eastern Mediterranean from 25000 to 5000 cal BP: Setting the environmental background for the evolution of human civilisation. *Quat Sci Rev* 25:1517–1541.
8. Weninger B, et al. (2006) Climate forcing due to the 8200 cal yr BP event observed at Early Neolithic sites in the eastern Mediterranean. *Quat Res* 66(3):401–420.
9. Bar-Matthews M, Ayalon A (2011) Mid-Holocene climate variations revealed by high-resolution speleothem records from Soreq Cave, Israel and their correlation with cultural changes. *Holocene* 21(1):163–171.
10. Finné M, Holmgren K, Sundqvist HS, Weiberg E, Lindblom M (2011) Climate in the eastern Mediterranean, and adjacent regions, during the past 6000 years: A review. *J Archaeol Sci* 38(12):3153–3173.
11. Roberts N, Brayshaw D, Kuzucuoglu C, Perez R, Sadori L (2011) The mid-Holocene climatic transition in the Mediterranean: Causes and consequences. *Holocene* 21(1): 3–13.
12. Weiss H, et al. (1993) The genesis and collapse of third millennium north mesopotamian civilization. *Science* 261(5124):995–1004.
13. Dalfes HN (1997) Environmental vulnerability of early societies: some reflections on modeling issues. *Third Millennium BC Climate Change and Old World Collapse,* NATO ASI Series I, eds Dalfes HN, Kukla G, Weiss H (Springer, Berlin), Vol 49, pp 691–698.
14. Cullen HM, et al. (2000) Climate change and the collapse of the Akkadian empire: Evidence from the deep sea. *Geology* 28(4):379–382.
15. Staubwasser M, Weiss H (2006) Holocene climate and cultural evolution in late prehistoric-early historic West Asia. *Quat Res* 66:372–387.
16. Kuzucuoglu C, Marro C, eds (2007) *Sociétés Humaines et Changement Climatique à la Fin du Troisième Millénaire: Une Crise a-t-Elle eu Lieu en Haute Mésopotamie*? (Diffusion De Boccard, Paris), Vol XIX.
17. Wilkinson TJ (1997) Environmental fluctuations, agricultural production and collapse: A view from Bronze Age upper Mesopotamia. *Third Millennium BC Climate Change and Old World Collapse,* NATO ASI Series I, eds Dalfes HN, Kukla G, Weiss H (Springer, Berlin), Vol 49, pp 67–106.
18. Wilkinson TJ (2004) *On the Margin of the Euphrates: Settlement and Land Use at Tell es-Sweyhat and the Upper Lake Assad Area, Syria* (Oriental Institute, Chicago).
19. Riehl S (2009) Archaeobotanical evidence for the interrelationship of agricultural decision-making and climate change in the ancient Near East. *Quat Int* 197:93–114.
20. Kaniewski D, Van Campo E, Weiss H (2012) Drought is a recurring challenge in the Middle East. *Proc Natl Acad Sci USA* 109(10):3862–3867.
21. Araus JL, et al. (1997) Changes in carbon isotope discrimination in grain cereals from different regions of the western Mediterranean basin during the past seven millenia: Palaeoenvironmental evidence of a differential change in aridity during the late Holocene. *Glob Change Biol* 3:107–118.
22. Ferrio JP, Araus JL, Buxó R, Voltas J, Bort J (2005) Water management practices and climate in ancient agriculture: Inferences from the stable isotope composition of archaeobotanical remains. *Veg Hist Archaeobot* 14:510–517.
23. Riehl S, Bryson RA, Pustovoytov K (2008) Changing growing conditions for crops during the Near Eastern Bronze Age (3000-1200 BC): The stable carbon isotope evidence. *J Archaeol Sci* 35(4):1011–1022.
24. Fiorentino G, et al. (2008) Third millennium B.C. climate change in Syria highlighted by Carbon stable isotope analysis of 14C-AMS dated plant remains from Ebla. *Palaeogeogr Palaeoclimatol Palaeoecol* 266(1-2):51–58.
25. Aguilera M, Ferrio JP, Pérez G, Araus JL, Voltas J (2012) Holocene changes in precipitation seasonality in the western Mediterranean Basin: A multi-species approach using δ13C of archaeobotanical remains. *J Quaternary Sci* 27(2):192–202.
26. Caracuta V, Fiorentino G, Martinelli MC (2012) Plant remains and AMS: Dating climate change in the Aeolian Islands (North Eastern Sicily) during the 2nd millennium BC. *Radiocarbon* 54(2-3):689–700.
27. Hartman G, Danin A (2010) Isotopic values of plants in relation to water availability in the Eastern Mediterranean region. *Oecologia* 162(4):837–852.
28. Stewart GR, Turnbull MH, Schmidt S, Erskine PD (1995) 13C natural abundance in plant communities along a rainfall gradient: A biological intergrator of water availability. *Aust J Plant Physiol* 22:51–55.
29. Araus JL, et al. (1999) Crop water availability in early agriculture: Evidence from carbon isotope discrimination of seeds from a tenth millennium BP sites on the Euphrates. *Glob Change Biol* 5:201–212.
30. Riehl S (2010) Maintenance of agricultural stability in a changing environment: The archaeobotanical evidence at Emar. *Late Roman and Medieval Cemeteries and Environmental Studies.* Emar After the Closure of the Tabqa Dam: The Syrian-German excavations 1996–2002, Subartu Book 25, eds Finkbeiner U, Sakal F (Brepols, Turnhout, Belgium), Vol 1, pp 177–224.
31. Araus JL, et al. (1997) Identification of ancient irrigation practices based on the carbon isotope discrimination of plant seeds: A case study from the South-East Iberian Peninsula. *J Archaeol Sci* 24(8):729–740.
32. Riehl S (2008) Climate and agriculture in the ancient Near East: A synthesis of the archaeobotanical and stable carbon isotope evidence. *Veg Hist Archaeobot* 17(1):43–51.
33. Flohr P, Müldner G, Jenkins E (2011) Carbon stable isotope analysis of cereal remains as a way to reconstruct water availability: Preliminary results. *Water Hist* 3(2):121–144.
34. Kühne H (1990) The effects of irrigation agriculture: Bronze and Iron Age habitation along the Khabur, Eastern Syria. *Man's Role in the Shaping of the Eastern Mediterranean Landscape*, eds Bottema S, Entjes-Nieborg G, van Zeist W (Balkema, Rotterdam), pp 15–30.
35. Bond G, et al. (2001) Persistent solar influence on North Atlantic climate during the Holocene. *Science* 294(5549):2130–2136.
36. Haug GH, Hughen KA, Sigman DM, Peterson LC, Röhl U (2001) Southward migration of the intertropical convergence zone through the Holocene. *Science* 293(5533): 1304–1308.
37. Mayewski P, et al. (2004) Holocene climate variability. *Quat Res* 62:243–255.
38. Wanner H, et al. (2008) Mid- to Late Holocene climate change: An overview. *Quat Sci Rev* 27(19-20):1791–1828.
39. Hole F (1997) Evidence for Mid-Holocene environmental change in the western Khabur drainage, Northeastern Syria. *Third Millennium BC Climate Change and Old World Collapse,* NATO ASI Series I, eds Dalfes HN, Kukla G, Weiss H (Springer, Berlin), Vol 49, pp 39–66.
40. Vannière B, et al. (2011) Circum-Mediterranean fire activity and climate changes during the mid-Holocene environmental transition (8500-2500 cal. BP). *Holocene* 21(1):53–73.
41. Ur J (2012) Spatial scale and urban collapse at Tell Brak and Hamoukar at the end of the third millennium BC. *Looking North: The Socioeconomic Dynamics of Northern Mesopotamian and Anatolian Regions During the Late Third and Early Second Millennium BC*, eds Laneri N, Pfälzner P, Valentini S (Harrassovitz, Wiesbaden, Germany), pp 25–35.
42. Höflmayer F, Dee MW, Genz H, Riehl S (2014) Radiocarbon evidence for the Early Bronze Age Levant: The site of Tell Fadous-Kfarabida (Lebanon) and the end of the Early Bronze III period. *Radiocarbon* 56(2):1–14.
43. Sandweiss DH, Maasch KA, Anderson DG (1999) Transitions in the Mid-Holocene. *Science* 283(5401):499–500.
44. Riehl S, Pustovoytov KE, Hotchkiss S, Bryson RA (2009) Local Holocene environmental indicators in Upper Mesopotamia: Pedogenic carbonate record vs. archaeobotanical data and archaeoclimatological models. *Quat Int* 209:154–162.
45. Roberts N, Eastwood WJ, Kuzucuoglu C, Fiorentino G, Caracuta V (2011) Climatic, vegetation and cultural change in the eastern Mediterranean during the mid-Holocene environmental transition. *Holocene* 21(1):147–162.
46. Wilkinson TJ, et al. (2014) Contextualizing early urbanization: Settlement cores, early states and agro-pastoral strategies in the Fertile Crescent during the fourth and third millennia BC. *J World Prehist* 27:43–109.
47. Araus JL, Ferrio JP, Buxó R, Voltas J (2007) The historical perspective of dryland agriculture: Lessons learned from 10,000 years of wheat cultivation. *J Exp Bot* 58(2): 131–145.
48. Geyer B, et al. (2007) The arid margins of northern Syria: Occupation of the land and modes of exploitation in the Bronze Age. *Urban and Natural Landscapes of an Ancient Syrian Capital: Settlement and Environment at Tell Mishrifeh/Qatna and in Central-Western Syria*, ed Bonacossi DM (Forum, Udine, Italy), pp 269–339.
49. Cremaschi M, Trombino L, Sala A, Valsecchi V (2003) Under fitted streams and the Holocene palaeo-environment in the region of Tell Mishrifeh-Qatna (Central Syria). *Akkadica* 124(1):71–77.
50. Litt T, et al. (2009) 'PALEOVAN', International Continental Scientific Drilling Program (ICDP): Site survey results and perspectives. *Quat Sci Rev* 28:1555–1567.
51. Langgut D, Finkelstein I, Litt T (2013) Climate and the Late Bronze collapse: New evidence from the southern Levant. *Tel Aviv* 40:149–175.
52. Kuzucuoğlu C, Dörfler W, Kunesch S, Goupille F (2011) Mid- to late-Holocene climate change in central Turkey: The Tecer Lake record. *Holocene* 21(1):173–188.
53. Heaton THE, Jones G, Halstead P, Tsipropoulos T (2009) Variations in the 13C/12C ratios of modern wheat grain, and implications for interpreting data from Bronze Age Assiros Toumba, Greece. *J Archaeol Sci* 36(10):2224–2233.
54. Barnola JM, Raynaud D, Korotkevich YS, Lorius C (1987) Vostok ice core provides 160,000-year record of atmospheric CO_2. *Nature* 329:408–414.
55. Wagner F, Bohncke SJ, Dilcher DL, Kurschner WM, van Geel B, Visscher H (1999) Century-scale shifts in early holocene atmospheric CO2 concentration. *Science* 284(5422):1971–1973.
56. Indermühle A, Stauffer B, Stocker TF, Raynaud D, Barnola J-M (1999) Early Holocene atmospheric CO2 concentrations. *Science* 286(5446):1815.
57. Ferrio JP, Voltas J, Araus JL (2012) A smoothed curve of $\delta^{13}C$ of atmospheric CO_2 from 16.100 BCE to 2.010 CE. Available at http://web.udl.es/usuaris/x3845331/AIRCO2_LOESS.xls. Accessed February 20, 2014.
58. Ferrio JP, Voltas J, Araus JL (2003) Use of carbon isotope composition in monitoring environmental changes. *Manage Environ Qual* 14(1):82–98.
59. Moran PAP (1950) Notes on continuous stochastic phenomena. *Biometrika* 37(1-2): 17–23.
60. Burrough PA, McDonnell R (1998) *Principles of Geographic Information Systems* (Oxford Univ Press, Oxford).
61. Conolly J, Lake M (2006) *Geographical Information Systems in Archaeology* (Cambridge Univ Press, Cambridge, UK).
62. Terzopoulos D (1988) The computation of visible-surface representations. *IEEE Trans Pattern Anal Mach Intell* 10(4):417–438.
63. Burns ER, Morgan DS, Peavler RS, Kahle SC (2011) *Three-Dimensional Model of the Geologic Framework for the Columbia Plateau Regional Aquifer System, Idaho, Oregon, and Washington* (US Geological Survey, Reston, VA), Scientific Investigations Report 2010-5246, p 44.
64. Berenbrock C, Mason RR, Jr, Blanchard SF (2009) Mapping Hurricane Rita inland storm tide. *J Flood Risk Manage* 2:76–82.